Identification, pharmacological evaluation and binding mode analysis of novel chromene and chromane based σ1 receptor ligands

ARTICLE *in* EUROPEAN JOURNAL OF MEDICINAL CHEMISTRY · AUGUST 2014

Impact Factor: 3.45 · DOI: 10.1016/j.ejmech.2014.06.054

7 AUTHORS, INCLUDING:

Domenico Marson
Università degli Studi di Trieste
9 PUBLICATIONS **64** CITATIONS
SEE PROFILE

Dirk Schepmann
University of Münster
101 PUBLICATIONS **1,027** CITATIONS
SEE PROFILE

Thomas J. Schmidt
University of Münster
142 PUBLICATIONS **2,907** CITATIONS
SEE PROFILE

Sabrina Pricl
Università degli Studi di Trieste
247 PUBLICATIONS **3,775** CITATIONS
SEE PROFILE

European Journal of Medicinal Chemistry 83 (2014) 526–533

Contents lists available at ScienceDirect

European Journal of Medicinal Chemistry

journal homepage: http://www.elsevier.com/locate/ejmech

Original article

Identification, pharmacological evaluation and binding mode analysis of novel chromene and chromane based σ_1 receptor ligands

Erik Laurini [a, 1], Dipak Harel [b, 1], Domenico Marson [a], Dirk Schepmann [b], Thomas J. Schmidt [c], Sabrina Pricl [a, **, 2], Bernhard Wünsch [b, d, *, 2]

[a] MOSE-DEA, University of Trieste, Piazzale Europa 1, 34127 Trieste, Italy
[b] Institut für Pharmazeutische und Medizinische Chemie der Westfälischen Wilhelms-Universität Münster, Corrensstraße 48, D-48149 Münster, Germany
[c] Institut für Pharmazeutische Biologie und Phytochemie der Westfälischen Wilhelms-Universität Münster, Corrensstraße 48, D-48149 Münster, Germany
[d] Cells-in-Motion Cluster of Excellence (EXC 1003 – CiM), University Münster, Germany

ARTICLE INFO

Article history:
Received 11 April 2014
Received in revised form
23 June 2014
Accepted 25 June 2014
Available online 26 June 2014

Keywords:
Molecular interactions
σ_1 receptor ligands
Structure affinity relationships
Docking studies
Molecular dynamics simulations
Binding pose

ABSTRACT

A set of aminoethyl substituted chromenes **3** and chromanes **4**, originally developed as antiprotozoal drugs was evaluated as novel types of σ_1 receptor ligands. Analysis of SAR showed that chromenes **3** have a higher σ_1 affinity than chromanes **4**. A distance of four bond lengths between the basic amino moiety and the phenyl ring (**3c**), an alicyclic N-substituent such as the cyclohexylmethyl moiety (**3l**), and methylation of the secondary amine to afford a tertiary amine (**3n**) result in very high σ_1 affinity and selectivity over the σ_2 subtype. Compounds **3a**–**n** and **4a**–**e** were docked into the putative binding site of the σ_1 receptor model and the relevant binding mode was analyzed and scored. Specifically, for the best σ_1 ligand **3n**, a salt bridge between Asp126 and the protonated amino group, an H-bond between the receptor backbone NH group (Ala122–Glu123) and the methoxy moiety of **3n**, a lipophilic protein cavity encasing the chromene ring, and a T-shaped π–π stacking between the indole ring of Trp121 and the phenyl ring of **3n** represent the most important ligand/protein stabilizing interactions. The binding pose of **3n** was compared with the binding poses of the non-methylated chromene **3c**, the saturated chromane **4c**, and the N-cyclohexylmethyl derivative **3l**. The contribution of the single amino acids to the overall free binding enthalpy was analyzed.

1. Introduction

In the mid-1970s σ receptors were discovered and proposed as a new class of opioid receptors [1]. Since the effects of typical σ ligands could not be reversed by opioid receptor antagonists such as naloxone and naltrexone [2,3], the σ receptor was removed from the class of opioid receptors. Today, it is well established that σ receptors represent unique binding sites without any homology with opioid receptors. Two subtypes of the σ receptor have been identified, termed σ_1 and σ_2 receptor, respectively [4,5].

The human σ_1 receptor has been cloned. Its gene encodes for a protein of 223 amino acids [6], which resides predominantly in the endoplasmic reticulum (ER) membrane, in the mitochondria-associated ER membrane (MAM), and the plasma membrane [7]. The σ_1 receptor acts as ligand-regulated molecular chaperone [8,9] that modulates the activity of several ion channels (Ca^{2+}, K^+ channels) [10–13] and receptors such as the *N*-methyl-D-aspartate (NMDA) receptor [14]. Nonselective σ_1 ligands have been assayed in clinical studies for the treatment of depression, psychosis and drug abuse [15–18]. Very recently, S1RA (**1**, Fig. 1) has entered phase II clinical trials for the treatment of neuropathic pain [19–22].

According to the pharmacophore model developed by Glennon et al. potent σ_1 ligands should contain a basic amino group flanked by two hydrophobic structural elements at defined distances [23–25]. Various prototypical σ_1 agonists such as (+)-pentazocine and NE100 as well as prototypical σ_1 antagonists such as spirocyclic piperidines and haloperidol (**2**) follow this model [26–29]. However, the σ_1 antagonist S1RA (**1**) does not contain a second hydrophobic moiety to occupy the secondary hydrophobic region as

* Corresponding author. Institut für Pharmazeutische und Medizinische Chemie der Westfälischen Wilhelms-Universität Münster, Corrensstraße 48, D-48149 Münster, Germany.
** Corresponding author. MOSE-DEA, University of Trieste, Piazzale Europa 1, 34127 Trieste, Italy.
E-mail address: wuensch@uni-muenster.de (B. Wünsch).
[1] These authors equally contributed to this work.
[2] Senior co-authors.

http://dx.doi.org/10.1016/j.ejmech.2014.06.054
0223-5234/

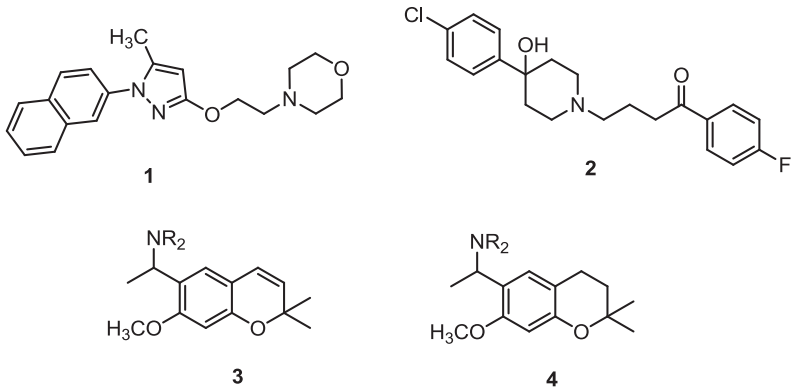

Fig. 1. The σ_1 receptor antagonists S1RA (**1**), haloperidol (**2**), and the general structure of chromenes **3** and chromanes **4** derived from the natural product encecalin.

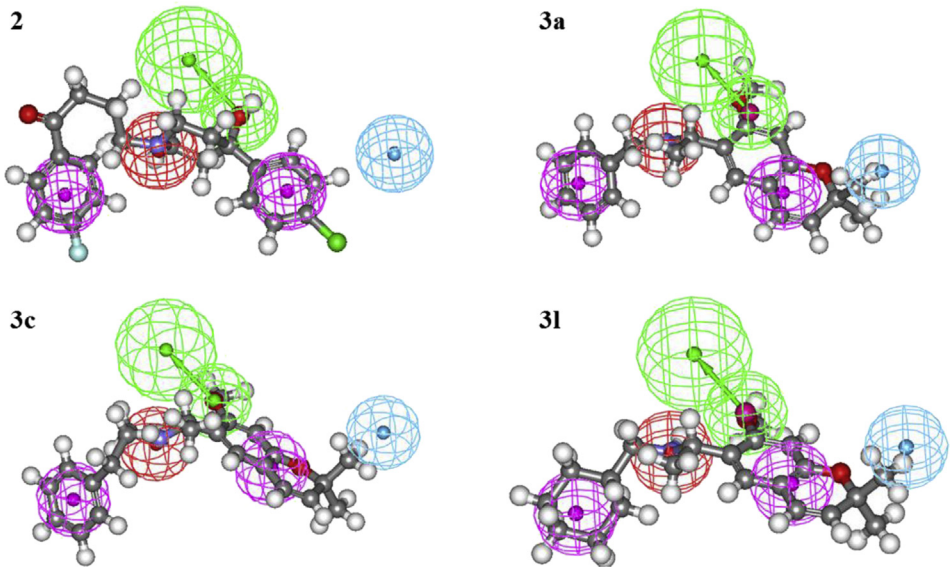

Fig. 2. Mapping of compounds **2**, **3a**, **3c**, and **3l** onto the σ_1 3D pharmacophore model developed for spirocyclic piperidines [35]. The hypothesis features are portrayed as meshed spheres, color-coded as follows: red, Positive Ionizable; light blue, Hydrophobic Aromatic; pink, Hydrophobic; light green, H-Bond Acceptor. Compounds are portrayed as atom-colored balls-and-sticks (red, O; yellow, S; gray, C; blue, N; white, H). (For interpretation of the references to colour in this figure legend, the reader is referred to the web version of this article.)

postulated by the pharmacophore model. A careful analysis of the binding mode of S1RA showed that, even in the absence of this pharmacophoric requirement, substantial stabilizing interactions with the σ_1 receptor exist. Additionally, exposition of the polar morpholine ring to the polar solvent contributes favorably to the free binding enthalpy due to low desolvation energy required for binding [30].

The σ_2 receptor still remains to be cloned and characterized unambiguously. Very recently it has been proposed that the progesterone receptor membrane component 1 (pgrmc1), which binds directly the heme group and regulates lipid and drug metabolism and hormone signaling, represents the σ_2 receptor binding site [31]. It has been reported that σ_2 receptor ligands can be used as biomarkers for tumor cell proliferation and to induce apoptosis. Therefore they could be exploited for tumor imaging and treatment [32]. Since the pharmacology of σ_1 and σ_2 receptors is clearly differentiated, ligands selectively addressing a single σ receptor subtype are of high interest for the development of a profound understanding of the complete σ receptor system.

Recently, we reported the synthesis and antiprotozoal activity of chromene **3** and chromanes **4** derived from the natural product encecalin [33,34]. Both series of compounds are characterized by a basic amino group linked to an ethyl side chain at position 6 of the heterocyclic system (Fig. 1). Mapping **3** and **4** onto the σ_1 pharmacophore model of Glennon led to a good correlation: the basic amino moiety of **3** and **4** is flanked by the chromene or chromane system as primary hydrophobic group while the lipophilic N-substituent represents the second hydrophobic group occupying the

Table 1
$K_{i(est)}$ values for compounds **2**, **3a**, **3c**, and **3l** for the σ_1 receptor estimated on the basis of the pharmacophore hypothesis.

Compd.	NR_2	$K_{i(est)}$ (nM)
2	–	20
3a	NH–CH_2Ph	13
3c	NH–$CH_2CH_2CH_2$Ph	10
3l	NH–$CH_2C_6H_{11}$	9.7

alternative hydrophobic region of the receptor. The third substituent at the amino moiety is either a proton or a small methyl group. Given these premises we then decided to analyze chromenes **3** and chromanes **4** as σ_1 receptor ligands.

2. Results and discussion

2.1. 3D pharmacophore model-based criterion for testing compounds 3 and 4 as σ_1 ligands

Given the presence in their molecular scaffold of the typical pharmacophores required for σ_1 receptor binding, and the structural similarity between the chromenes **3** and chromanes **4** and the σ_1 receptor ligands **1** and **2**, we decided to test molecules **3** and **4** as potential σ_1 binders. To this purpose, as a proof of concept we firstly mapped compounds **2**, **3a**, **3c**, and **3l** onto our 3D pharmacophore model for σ_1 subtype ligands recently developed for rationalizing the σ_1 affinity of spirocyclic piperidines [35]. Although the hydrophobic aromatic feature remains unmapped by all molecules (Fig. 2), the excellent overlay between the molecular chemical moieties and all remaining 3D pharmacophoric features resulted in the interesting predicted σ_1 affinity reported in Table 1. Notably, the σ_1 affinity predicted for haloperidol (**2**) ($K_{i(est)}$ = 20 nM) is in agreement with the experimental value (K_i = 6.3 nM).

2.2. Synthesis of compounds 3 and 4

Briefly, the aminoethyl substituted chromenes **3** and chromanes **4** were prepared from the common intermediate **6**, which was obtained in two reaction steps form commercially available resorcinol (**5**). (Scheme 1) Methylation, reductive amination using different amines with or without DDQ oxidation as first step converted the ketone **6** into chromenes **3** and chromanes **4**, respectively [33]. Ellman's chiral sulfinamide served as chiral auxiliary in the synthesis of enantiomerically pure *N*-benzylamines (*R*)- and (*S*)-**3a** and *N*-methyl-*N*-benzylamines (*R*)- and (*S*)-**3o** [34].

2.3. Relationships between the structure of chromenes 3 and chromanes 4 and their σ_1 and σ_2 receptor affinities

The σ_1 and σ_2 receptor affinity of the chromenes **3** and chromanes **4** was determined in receptor binding studies employing the radioligands [^{3}H]-(+)-pentazocine and [^{3}H]-di-*o*-tolylguanidine, respectively. An excess of (+)-pentazocine was added in the σ_2 assay to mask the σ_1 binding sites, thus avoiding their labeling by [^{3}H]-di-*o*-tolylguanidine. Membrane preparations generated from guinea pig brains and rat liver served as receptor material in the σ_1 and σ_2 assays, respectively [36,37].

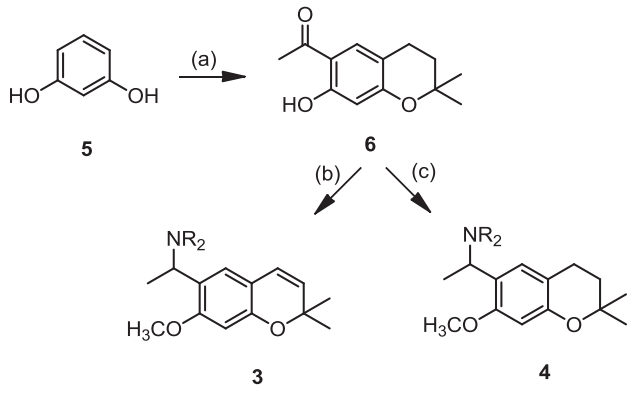

Scheme 1. Synthesis of chromenes **3** and chromanes **4** via ketone **6**. (a) 2 steps (formation of chromane, acetylation) [33]. (b) 3 steps (DDQ oxidation, methylation, reductive amination) [33]. (c) 2 steps (methylation, reductive amination) [33].

The homologous phenylalkylamines **3a**–**d** with a chromene scaffold show slightly higher σ_1 affinity than the corresponding chromane-based compounds **4a**–**d**. (Table 2) In both molecular series the σ_1 affinity increased by increasing the number of methylene groups between the phenyl ring and the basic amino moiety, reaching a maximum of σ_1 affinity for the 3-phenylpropylamines **3c** (K_i = 11 nM) and **4c** (K_i = 19 nM). The phenylbutylamines **3d** and **4d** show reduced σ_1 affinity compared to the phenylpropylamines **3c** and **4c**.

Due to its low σ_2 affinity the phenylpropylamine **3c** displayed very high σ_1/σ_2-selectivity (77 fold). In the series of homologous phenylalkylamines **3a**–**d** the phenylethylamine **3b** was endowed with the highest σ_2 affinity (K_i = 152 nM), although **3b** still shows a five-fold selectivity for the σ_1 subtype.

The presence of a methoxy moiety in the benzylamine **3a** led to **3e**, characterized by decreased σ_1 and increased σ_2 affinity. Altogether, the *p*-methoxybenzylamine **3e** represents a non-selective σ receptor ligand. A reduced σ_1 affinity was also observed after introduction of a methyl moiety at the α-position of the benzyl moiety. Interestingly, the configuration of the chiral center in benzylic position has only a small influence on the σ_1 affinity (compare **3g** and **3h**).

Table 2
σ_1 and σ_2 affinities of aminoethyl substituted chromenes **3a**–**o** and chromanes **4a**–**e** compared with the σ affinities of reference compounds. The experiments were recorded in triplicates (n = 3).

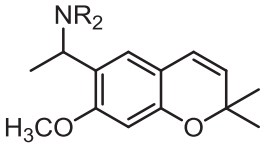

3a-o

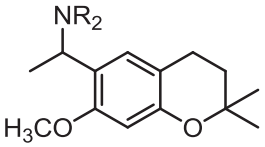

4a-e

Compd.	NR_2	K_i ± SEM [nM]		σ_1/σ_2-selectivity
		σ_1	σ_2	
3a	NH–CH_2Ph	75 ± 23	2290	30
(*R*)-**3a**	NH–CH_2Ph	112 ± 33	23%[a]	>10
(*S*)-**3a**	NH–CH_2Ph	85 ± 9.0	1600	19
3b	NH–CH_2CH_2Ph	29 ± 16	152	5
3c	NH–$CH_2CH_2CH_2$Ph	11 ± 1.8	850	77
3d	NH–$CH_2CH_2CH_2CH_2$Ph	37 ± 12	226	6
3e	NH–CH_2-4-MeOPh	165 ± 73	156	1
3f	NH–CH_2CH=CHPh	83 ± 28	348	4
3g	(*R*)–NH–$CH(CH_3)$Ph	232 ± 36	2380	10
3h	(*S*)–NH–$CH(CH_3)$Ph	805 ± 64	9260	12
3i	NH–CH_2CH_3	83 ± 26	noc[b]	–
3j	NH–$CH_2CH_2CH_2CH_3$	22 ± 8.0	1080	49
3k	NH–$CH(CH_3)(CH_2)_3NEt_2$	192 ± 61	1700	9
3l	NH–$CH_2C_6H_{11}$	2.4 ± 1.2	128	53
3m	$N(CH_2CH_2)_2$	19 ± 5	378	20
3n	$N(CH_3)$–$CH_2CH_2CH_2$Ph	0.95 ± 0.2	540	568
(*R*)-**3o**	$N(CH_3)$–CH_2Ph	4.5 ± 1.1	1250	250
(*S*)-**3o**	$N(CH_3)$–CH_2Ph	2.8 ± 0.7	343	123
4a	$NHCH_2$Ph	119 ± 66	2180	18
4b	NH–CH_2CH_2Ph	55 ± 26	1400	25
4c	NH–$CH_2CH_2CH_2$Ph	19 ± 2	292	15
4d	NH–$CH_2CH_2CH_2CH_2$Ph	115 ± 42	133	2
4e	NH–$CH_2CH_2CH_2CH_3$	43 ± 18	972	23
(+)-pentazocine		5.6 ± 2.2	–	–
Haloperidol		6.3 ± 1.6	78 ± 2.3	12
di-*o*-(tolyl)guanidine		89 ± 29	57 ± 18	0.7

[a] At a test compound concentration of 1 μM the radioligand binding was reduced only by 26%. Therefore the exact K_i value, which is at least higher than 1 μM, was not recorded.

[b] noc: a correlation between concentration and σ_2 affinity could not be found.

Conformational restriction of the side chain of the very potent phenylpropylamine **3c** by a *trans*-configured double bond (**3f**) led to 8-fold decreased σ_1 affinity and 2-fold increased σ_2 affinity.

An aliphatic substituent at the basic amino moiety should have a considerable size but should not contain an additional basic functional group (e.g. **3k**) to result in a potent σ_1 ligand. Thus the pyrrolidine **3m** and the butylamines **3j** and **4e** show higher σ_1 affinity than the smaller ethylamine **3i**, but lower σ_1 affinity than the larger cyclohexylmethylamine **3l** interacting in the low nanomolar range with the σ_1 receptor ($K_i = 2.4$ nM). Although the σ_2 affinity is also rather high ($K_i = 128$ nM), the cyclohexylmethylamine **3l** possesses a 53-fold selectivity for the σ_1 subtype.

N-methylation of the secondary amines **3a** and **3c** led to a dramatic increase of the σ_1 affinity. The σ_1 affinity of the methylated benzylamines (*R*)-**3o** and (*S*)-**3o** is 17- to 27-fold higher than the σ_1 affinity of **3a**, and the methylated phenylpropylamine **3n** is 11-fold more potent than **3c**. The methylated phenylpropylamine **3n** represents the most affine ($K_i = 0.95$ nM) and most selective ($\sigma_1/\sigma_2 = 568$) σ_1 ligand of both series of aminoethyl substituted chromenes and chromanes.

In order to analyze the effect of the configuration on the σ_1 receptor affinity the enantiomerically pure benzylamines (*R*)-**3a** and (*S*)-**3a** as well as the enantiomerically pure methylated benzylamines (*R*)-**3o** and (*S*)-**3o** were included in the tests. It was found that the enantiomers had very similar σ_1 affinity with an eudismic ratio <2, respectively, indicating low stereo-differentiation of the σ_1 receptor.

2.4. Molecular modeling studies

In order to confirm the σ_1 structure–affinity relationships presented above for all aminoethyl substituted chromene and chromane derivatives, compounds **3a**–**n** and **4a**–**e** were docked into the putative binding site of our σ_1 receptor model [38,39]. Then, each resulting receptor/ligand complex was relaxed by energy minimization followed by molecular dynamics (MD) simulations. Finally, the relevant values of the free energy of binding (ΔG_{bind}) between all compounds and the σ_1 receptor were evaluated by applying the molecular mechanics/Poisson–Boltzmann surface area (MM/PBSA) computational ansatz, as shown in Table 3.

As shown in Table 3, our methodology not only ranked the affinity to the σ_1 receptor of both compound series in the correct order, but also yielded $K_{i(est)}$ values in quantitative agreement with the experimentally determined values.

Considering chromene derivative **3n** as lead compound ($\Delta G_{bind} = -12.73$ kcal/mol, Table 3), we proceeded and analyzed the main interactions involved in the stabilization of the corresponding σ_1 receptor/**3n** complex. Specifically, we detected four key stabilizing interactions in the binding mode of **3n** (Fig. 3), which are in good agreement with the typical pharmacophore requirements previously reported for σ_1 ligands: i) a salt bridge between the carboxylic group in the side chain of Asp126 and the protonated N–CH_3 portion of ligand **3n**; ii) an H-bond between the acceptor methoxy substituent of **3n** and the donor –NH group belonging to the backbone peptidic bond between Ala122 and Glu123; iii) a network of stabilizing hydrophobic interactions via van der Waals forces between the chromene ring and the carbonic side chain of the receptor residues Ile128, Phe133, Tyr173 and Leu186 and iv) a T-shaped π–π stacking between the aromatic portion of Trp121 and the phenyl ring of **3n**.

A deconvolution of the enthalpic component (ΔH_{bind}) of the binding free energy on a per-residue basis led to the results shown in Fig. 4(A). Substantially, the permanent salt bridge between the protonated N-atom of **3n** and the side chain of Asp126 (average dynamic length (ADL) = 3.85 ± 0.06 Å) reflects in a stabilizing contribution of −2.83 kcal/mol. Concomitantly, the stable hydrogen bond (ADL = 1.92 ± 0.07 Å) involving the ether O atom of **3n** and the donor NH group of the peptidic bond between Ala122 and Glu123 yields a favorable contribution of −1.81 kcal/mol. Moreover, the hydrophobic interactions between the chromene ring of **3n** and the side chains of residues Ile128, Phe133, Tyr173, and Leu186 contribute an overall stabilization term to binding equal to −5.24 kcal/mol. Finally, the important T-stacking π–π interaction established between the phenyl ring of **3n** and the indole ring of Trp121 results in a strong enthalpic stabilization of −2.33 kcal/mol.

Table 3
Estimated free binding energies ΔG_{bind} (kcal/mol) and $K_{i(est)}$ values for the entire set of chromenes **3** and chromanes **4** in complex with the σ_1 receptor. The corresponding experimental K_i values are also reported for comparison. Errors are given in parenthesis as standard errors of the mean. $K_{i(est)}$ were obtained from ΔG_{bind} using the relationship: $\Delta G_{bind} = -RT \ln(1/K_{i(est)})$.

Compd.	ΔG_{bind} (kcal/mol)	K_i (nM)	$K_{i(exp)}$ (nM)
3a	−9.39 (0.28)	132	75 (22)
3b	−9.99 (0.32)	48	29 (16)
3c	−10.48 (0.36)	21	11 (1.8)
3d	−9.45 (0.33)	119	37 (12)
3e	−9.17 (0.29)	189	165 (73)
3f	−9.06 (0.32)	230	83 (28)
3g	−8.67 (0.32)	440	232 (36)
3h	−8.66 (0.36)	450	805 (64)
3i	−9.19 (0.30)	185	83 (26)
3j	−9.68 (0.31)	68	22 (8)
3k	−8.18 (0.29)	1020	192 (61)
3l	−11.38 (0.35)	4.6	2.4 (1.2)
3m	−9.87 (0.35)	58	19 (5)
3n	−12.71 (0.28)	0.48	0.95 (0.2)
4a	−9.26 (0.34)	163	119 (61)
4b	−9.72 (0.36)	76	55 (26)
4c	−10.25 (0.32)	31	19 (2)
4d	−9.58 (0.32)	96	115 (42)
4e	−9.79 (0.36)	67	43 (18)

The same analysis was extended to all chromene and chromane derivatives **3** and **4**, with the aim of dissecting the main structural features responsible for similar and different σ_1 affinity of both series of compounds. The most important requirement to achieve a tailor-fitted binding mode within the σ_1 binding site seems to be the presence of a methyl group on the basic N-atom: indeed, the most favorable free energy of binding of **3n** can be attributed to its optimized conformation for binding in comparison with the non-methylated analogue **3c**, as shown in Fig. 4(B). Although the

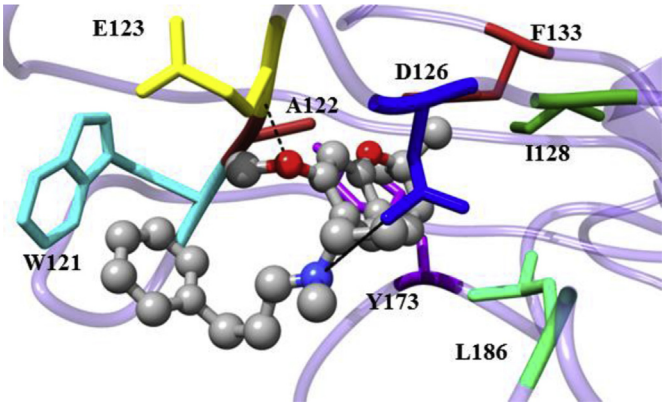

Fig. 3. Zoomed view of the σ_1 receptor in complex with **3n**. The compound is in atom-colored sticks-and-balls (red, O; blue, N; gray, C). Hydrogen atoms, water molecules, ions and counterions are not shown for clarity. Salt bridge and hydrogen bond interactions are highlighted with continuous and dashed black lines, respectively. (For interpretation of the references to colour in this figure legend, the reader is referred to the web version of this article.)

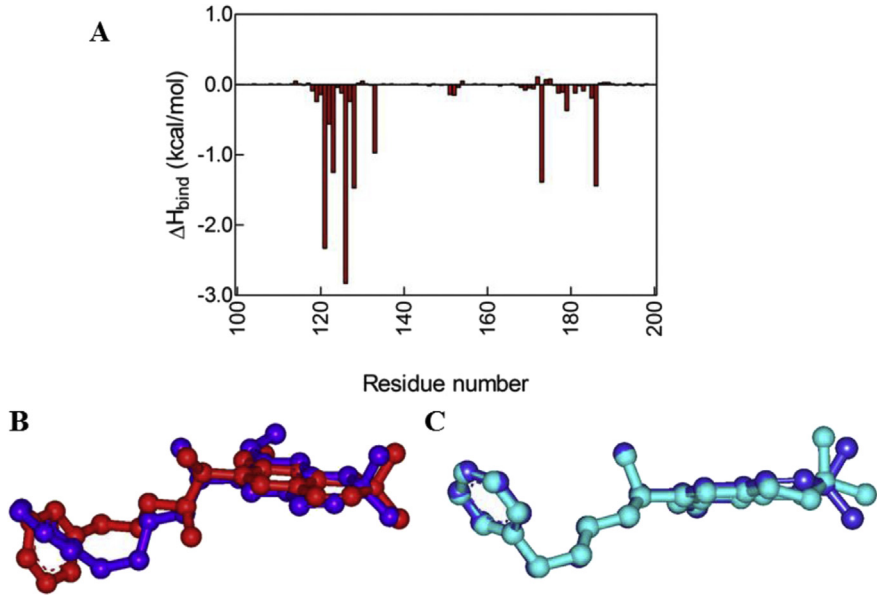

Fig. 4. (A) Per residue enthalpic contribution to binding for the σ_1/**3n** complex. Only amino acids from position 100 to 200 of the σ_1 receptor are shown, as for all remaining residues the contribution to ligand binding is irrelevant. (B) Comparison of the optimized conformations of compounds **3c** (blue) and **3n** (red) in the σ_1 binding site. (C) Comparison of the optimized conformations of compounds **3c** (blue) and **4c** (cyan) in the σ_1 binding site. (For interpretation of the references to colour in this figure legend, the reader is referred to the web version of this article.)

chromene scaffold of **3c** is perfectly encased in the hydrophobic portion of the σ_1 receptor binding pocket (mainly involving residues Ile128, Phe133, Tyr173, and Leu186), the phenyl ring of this compound is not able to adopt the same, optimal orientation as seen for **3n**. This, in turn, results both in a significant decrease in the efficacy of the π–π interaction with Trp121 (−1.16 kcal/mol instead of −2.33 kcal/mol) and in a less stable hydrogen bond formed by the peptide bond Ala122–Glu123 (−1.31 kcal/mol instead of −1.81 kcal/mol), as summarized in Table 4. Also in the case of the chromane derivative **4c** the phenyl moiety adopts a non-optimal configuration in the binding site (Fig. 4(C)), and the confined difference in the binding affinity with respect to **3n** can be ascribed to an overall, slightly less favorable adaptation of the chromane moiety to the receptor hydrophobic pocket (Table 4).

In principle, replacement of the phenylalkylamino group with an aliphatic side chain in compounds **3i**–**m** and **4e** should result in decreased σ_1 affinity for these compounds due to the missing, important π–π interaction with Trp121. Although a decrease of $K_{i(est)}$ is indeed predicted by our simulations (Fig. 5(A)), the non-negligible σ_1 affinity of these compounds can be explained by their rather different binding pose. As shown in Fig. 5(B) for the cyclohexylmethyl derivative **3l**, the lack of the aromatic interaction can be at least partially compensated by the establishment of a small, favorable hydrophobic network with the side chains of Ile178 and Leu182 (−0.89 and −0.95 kcal/mol, respectively).

However, as inferred from Fig. 5(A), the contribution of all other binding site residues to the stabilization of the σ_1 receptor/**3l** complex is lower than in the complex of the lead compound **3n**, thereby confirming the optimal conformation adopted by the N-methyl derivative **3n** upon binding to the receptor.

In order to describe a possible influence of the configuration on σ_1 receptor binding, MM/PBSA calculations were further exploited to estimate the affinity of (*R*)-**3a**, (*S*)-**3a**, (*R*)-**3o** and (*S*)-**3o** for the σ_1 receptor (Table 5). According to our simulations, both enantiomers of compounds **3a** and **3o** are endowed with comparable affinities towards the σ_1 receptor, as quantified by negligible differences in the corresponding ΔG_{bind} values. Moreover, the same network of stabilizing interactions with the σ_1 protein described for **3a** and **3o** are identified along the molecular dynamics trajectories of the corresponding enantiomer/σ_1 receptor complexes, regardless of the stereochemistry of the compounds (Fig. 6). Therefore, both (*R*)- and (*S*)-configured enantiomers of **3a** and **3o** can be accommodated within the σ_1 binding pocket without inducing any conformational alteration, whilst the aforementioned SAR considerations proposed to explain the difference of affinity between **3a** and **3o** still hold in the case of the separate enantiomers in complex with the σ_1 receptor.

Table 4
Per residue binding enthalpy contribution of the key binding amino acids for compounds **3c**, **3n** and **4c** in complex with σ_1 receptor.

Compd.	ΔG_{bind} (kcal/mol)	ΔH_{bind} (kcal/mol)							
		W121	A122	E123	D126	I128	F133	Y173	L186
3n	−12.71	−2.33	−0.56	−1.25	−2.83	−1.47	−0.97	−1.39	−1.44
3c	−10.48	−1.16	−0.39	−0.92	−2.78	−1.53	−0.92	−1.41	−1.30
4c	−10.25	−1.12	−0.42	−0.93	−2.71	−1.40	−0.88	−1.29	−1.22

3. Conclusion

Aminoethyl substituted chromenes **3** and chromanes **4** were originally synthesized and optimized to obtain high antiplasmodial and antileishmanial activity [33]. Since we observed a direct relation between the chemical features of these compounds and the σ_1 receptor pharmacophoric ligand requirements, the σ affinity of chromenes **3** and chromanes **4** has been recorded and analyzed in detail. It was shown that the chromenes **3** represent high affinity and selective σ_1 receptor ligands. Three methylene moieties represent the optimal distance between the basic amino moiety and the phenyl residue. A particular high σ_1 receptor affinity of 0.95 nM was achieved after methylation to yield the tertiary amine **3n**. The calculated free binding energy of the σ_1 receptor/**3n** complex of −12.73 kcal/mol correlates nicely with the recorded σ_1 affinity. The key interactions stabilizing the σ_1 receptor/**3n** complex are a salt bridge (Asp126–R_3NH^+), an H-bond (Ala122–NH–-Gli123–OCH_3), a network of hydrophobic interactions (Ile128, Phe133, Tyr713, Leu 196 – chromene ring) and a T-shaped π–π

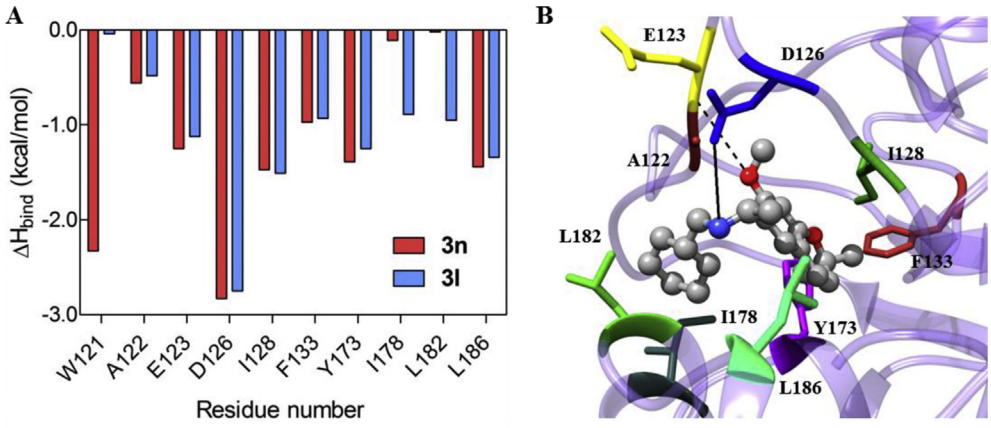

Fig. 5. (A) Per residue enthalpic contribution to binding for the σ_1/**3n** and σ_1/**3l** complex. Only σ_1 amino acids critical for the binding are shown. (B) Zoomed view of the σ_1 receptor in complex with **3l**. The compound is in atom-colored sticks-and-balls (red, O; blue, N; gray, C). Hydrogen atoms, water molecules, ions and counterions are not shown for clarity. Salt bridge and hydrogen bond interactions are highlighted with continuous and dashed black lines, respectively. (For interpretation of the references to colour in this figure legend, the reader is referred to the web version of this article.)

interaction (Trp121–phenyl ring). Differences in the binding mode of chromenes and chromanes, secondary and tertiary amines as well as phenylalkyl and cyclohexylmethyl residues were analyzed. The good correlation between the recorded K_i values and the calculated free binding energies supports nicely the 3D-homology model of the σ_1 receptor and its binding site.

4. Experimental part

4.1. Receptor binding studies

4.1.1. Materials

The guinea pig brains and rat liver for the σ_1 and σ_2 receptor binding assays were commercially available (Harlan-Winkelmann, Borchen, Germany). Homogenizer: Elvehjem Potter (B. Braun Biotech International, Melsungen, Germany). Cooling centrifuge model Rotina 35R (Hettich, Tuttlingen, Germany) and High-speed cooling centrifuge model Sorvall RC-5C plus (Thermo Fisher Scientific, Langenselbold, Germany). Multiplates: standard 96-well multiplates (Diagonal, Muenster, Germany). Shaker: self-made device with adjustable temperature and tumbling speed (scientific workshop of the institute). Vortex: Vortex Genie 2 (Thermo Fisher Scientific, Langenselbold, Germany). Harvester: MicroBeta FilterMate-96 Harvester. Filter: Printed Filtermat type A and B. Scintillator: Meltilex (type A or B) solid state scintillator. Scintillation analyzer: MicroBeta Trilux (all Perkin Elmer LAS, Rodgau-Jügesheim, Germany). Chemicals and reagents were purchased from different commercial sources and of analytical grade.

4.1.2. Preparation of membrane homogenates from guinea pig brain [36,37]

Five guinea pig brains were homogenized with the potter (500–800 rpm, 10 up-and-down strokes) in 6 volumes of cold 0.32 M sucrose. The suspension was centrifuged at 1200× g for 10 min at 4 °C. The supernatant was separated and centrifuged at 23,500× g for 20 min at 4 °C. The pellet was resuspended in 5–6 volumes of buffer (50 mM TRIS, pH 7.4) and centrifuged again at 23,500× g (20 min, 4 °C). This procedure was repeated twice. The final pellet was resuspended in 5–6 volumes of buffer and frozen (−80 °C) in 1.5 mL portions containing about 1.5 mg protein/mL.

4.1.3. Preparation of membrane homogenates from rat liver [36,37]

Two rat livers were cut into small pieces and homogenized with the potter (500–800 rpm, 10 up-and-down strokes) in 6 volumes of cold 0.32 M sucrose. The suspension was centrifuged at 1200× g for 10 min at 4 °C. The supernatant was separated and centrifuged at 31,000× g for 20 min at 4 °C. The pellet was resuspended in 5–6 volumes of buffer (50 mM TRIS, pH 8.0) and incubated at room temperature for 30 min. After the incubation, the suspension was centrifuged again at 31,000× g for 20 min at 4 °C. The final pellet

Table 5
Binding free energies ΔG_{bind} (kcal/mol) and $\sigma_1 K_{i(est)}$ for enantiomeric compounds **3a** and **3o** in complex with the σ_1 receptor. Errors are given in parenthesis as standard errors of the mean.

Compd.	ΔG_{bind} (kcal/mol)	$\sigma_1 K_{i(est)}$ (nM)	$\sigma_1 K_{i(exp)}$ (nM)
(*R*)-**3a**	−9.42 (0.29)	125	112 (33)
(*S*)-**3a**	−9.39 (0.28)	132	85 (9)
(*R*)-**3o**	−11.60 (0.30)	3.1	4.5 (1.1)
(*S*)-**3o**	−11.63 (0.32)	3.0	2.8 (0.7)

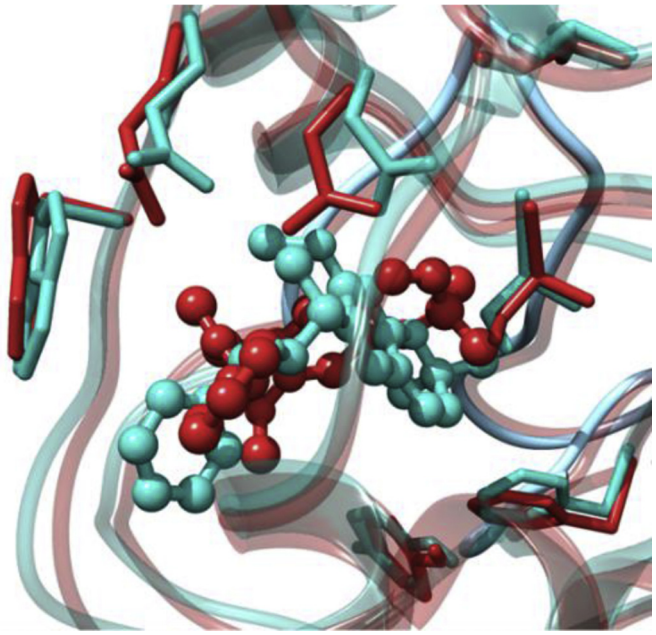

Fig. 6. Superposition of equilibrated MD snapshots of the σ_1 receptor in complex with (*R*)-**3a** (light sea green) and (*S*)-**3a** (firebrick). Hydrogen atoms, water molecules, ions and counterions are omitted for clarity. (For interpretation of the references to colour in this figure legend, the reader is referred to the web version of this article.)

was resuspended in 5–6 volumes of buffer and stored at −80,°C in 1.5 mL portions containing about 2 mg protein/mL.

4.1.4. Protein determination

The protein concentration was determined by the method of Bradford [40], modified by Stoscheck [41]. The Bradford solution was prepared by dissolving 5 mg of Coomassie Brilliant Blue G 250 in 2.5 mL of EtOH (95%, v/v). 10 mL deionized H_2O and 5 mL phosphoric acid (85%, m/v) were added to this solution, the mixture was stirred and filled to a total volume of 50.0 mL with deionized water. The calibration was carried out using bovine serum albumin as a standard in 9 concentrations (0.1, 0.2, 0.4, 0.6, 0.8, 1.0, 1.5, 2.0 and 4.0 mg/mL). In a 96-well standard multiplate, 10 μL of the calibration solution or 10 μL of the membrane receptor preparation were mixed with 190 μL of the Bradford solution, respectively. After 5 min, the UV absorption of the protein-dye complex at $\lambda = 595$ nm was measured with a platereader (Tecan Genios, Tecan, Crailsheim, Germany).

4.1.5. General protocol for the binding assays

The test compound solutions were prepared by dissolving approximately 10 μmol (usually 2–4 mg) of test compound in DMSO so that a 10 mM stock solution was obtained. To obtain the required test solutions for the assay, the DMSO stock solution was diluted with the respective assay buffer. The filtermats were presoaked in 0.5% aqueous polyethylenimine solution for 2 h at room temperature before use. All binding experiments were carried out in duplicates in 96-well multiplates. The concentrations given are the final concentrations in the assay. Generally, the assays were performed by addition of 50 μL of the respective assay buffer, 50 μL test compound solution in various concentrations (10^{-5}, 10^{-6}, 10^{-7}, 10^{-8}, 10^{-9} and 10^{-10} mol/L), 50 μL of corresponding radioligand solution and 50 μL of the respective receptor preparation into each well of the multiplate (total volume 200 μL). The receptor preparation was always added last. During the incubation, the multiplates were shaken at a speed of 500–600 rpm at the specified temperature. Unless otherwise noted, the assays were terminated after 120 min by rapid filtration using the harvester. During the filtration each well was washed five times with 300 μL of water. Subsequently, the filtermats were dried at 95 °C. The solid scintillator was melted on the dried filtermats at a temperature of 95 °C for 5 min. After solidifying of the scintillator at room temperature, the trapped radioactivity in the filtermats was measured with the scintillation analyzer. Each position on the filtermat corresponding to one well of the multiplate was measured for 5 min with the [^{3}H]-counting protocol. The overall counting efficiency was 20%. The IC_{50}-values were calculated with the program GraphPad Prism® 3.0 (GraphPad Software, San Diego, CA, USA) by non-linear regression analysis. Subsequently, the IC_{50} values were transformed into K_i-values using the equation of Cheng and Prusoff [42]. The K_i-values are given as mean value ± SEM from three independent experiments.

4.1.6. Protocol of the σ_1 receptor binding assay

The assay was performed with the radioligand [^{3}H]-(+)-pentazocine (22.0 Ci/mmol; Perkin Elmer). The thawed membrane preparation of guinea pig brain cortex (about 100 μg of protein) was incubated with various concentrations of test compounds, 2 nM [^{3}H]-(+)-Pentazocine, and TRIS buffer (50 mM, pH 7.4) at 37 °C. The non-specific binding was determined with 10 μM unlabeled (+)-Pentazocine. The K_d-value of (+)-pentazocine is 2.9 nM [43].

4.1.7. Protocol of the σ_2 receptor binding assay

The assays were performed with the radioligand [^{3}H]DTG (specific activity 50 Ci/mmol; ARC, St. Louis, MO, USA). The thawed membrane preparation of rat liver (about 100 μg of protein) was incubated with various concentrations of the test compound, 3 nM [^{3}H]DTG and buffer containing (+)-pentazocine (500 nM (+)-pentazocine in 50 mM TRIS, pH 8.0) at room temperature. The non-specific binding was determined with 10 μM non-labeled DTG. The K_d value of [^{3}H]DTG is 17.9 nM [44].

4.2. Molecular modeling

4.2.1. Molecular dynamics protocol

All molecular dynamics (MD) simulations and the relevant analyses were performed on the Amber 12 suites of programs [45] running on the Eurora-GPU and FERMI supercomputers at the CINECA supercomputer center (Bologna, Italy). Molecular graphics images were produced using UCSF Chimera [46]. Each σ_1/ligand complex was then allowed to relax in a 90 Å × 90 Å × 90 Å box of TIP3P water molecules [47]. The resulting system was minimized with a gradual decrease in the position restraints of the protein atoms. Finally, to achieve electroneutrality, a suitable number of neutralizing ions were added; further, the solution ionic strength was adjusted to the physiological value of 0.15 M by adding the required amounts of Na^+ and Cl^- ions. After energy minimization of the added ions for 1500 steps, keeping the protein, the ligand, and the pre-existing waters rigid, followed by an MD equilibration of the entire water/ion box with fixed solute for 2 ns, further unfavorable interactions within the structures were relieved by progressively smaller positional restraints on the solute for a total of 5 ns. Each hydrated complex system was gradually heated to 300 K in three intervals, allowing a 2 ns interval per each 100 K, and then equilibrated for 5 ns at 300 K, followed by 20 ns in canonical (NVT) ensemble of data production runs. The last 10 ns of each equilibrated MD trajectory were considered for statistical data collections, necessary for the estimation of the free energy of binding. The MD simulations were performed at constant $T = 300$ K using the Langevin thermostat [48], an integration time step of 2 fs, and the applications of the Shake algorithm [49] to constrain all bonds to their equilibrium values, thus removing high frequency vibrations. Long-range nonbonded van der Waals interactions were truncated by using a dual cutoff of 9 and 13 Å, respectively, where energies and forces due to interactions between 9 and 13 Å were updated every 20 time steps. The particle mesh Ewald method [50] was used to treat the long-range electrostatics. For the calculation of the binding free energy between σ_1 receptor and compounds **3a**–**n** and **4a**–**e** in water, a total of 1000 snapshots were saved during the MD data collection period described above.

4.2.2. MM/PBSA calculations

The binding free energy ΔG_{bind} of each σ_1/ligand complex in water was calculated according to the procedure termed Molecular Mechanic/Poisson–Boltzmann Surface Area (MM/PBSA), originally proposed by Srinivasan et al. [51]. The theoretical background of this methodology is described in details in the original papers by Peter Kollman and collaborators [52], and has been successfully employed by our group in related studies [53]. However, it is appropriate to describe it briefly below. Basically, an MD simulation (typically in explicit solvent) is first carried out which yields a representative ensemble of structures. The average total free energy of binding between each drug and the protein receptor can then be calculated as:

$$\Delta G_{blind} = \Delta E_{MM} + \Delta G_{solv} - T\Delta S \quad (1)$$

where ΔG_{bind} is the binding free energy in water, ΔE_{MM} is the interaction energy between ligand and σ_1 receptor, ΔG_{solv} is the solvation free energy, and $-T\Delta S$ is the conformational entropy

contribution to the binding. ΔE_{MM} is calculated from the molecular mechanics (MM) interaction energies, according to:

$$\Delta E_{MM} = \Delta E_{ele} + \Delta E_{vdw} \quad (2)$$

where ΔE_{ele} and ΔE_{vdw} are electrostatic and van der Waals interaction energies between the molecules and the biological target, which are calculated using the MM/PBSA module in the Amber 12 software suites.

The solvation energy, ΔG_{solv}, is divided into two parts, the electrostatic contributions, ΔG_{pol}, and all other contributions, ΔG_{nonpol}:

$$\Delta G_{solv} = \Delta G_{solv,pol} + \Delta G_{solv,nonpol} \quad (3)$$

The ΔG_{solv} is calculated using the MM/PBSA module in the Amber 12 software suites, which solves the Poisson–Boltzmann equations numerically and calculates the electrostatic energy according to the electrostatic potential. Interior and exterior dielectric constant values ε were set equal to 1 and 80, respectively.

The quasi-harmonic analysis [54] was then employed directly to obtain the last term in equation (1) i.e., the change in solute entropy upon association $-T\Delta S$, from the Cartesian-coordinate covariance matrix accumulated during the corresponding molecular dynamics trajectory. To minimize the effects due to different conformations adopted by individual snapshots we averaged the estimation of entropy over 100 snapshots.

Finally, the contribution of each σ_1 residue to the binding with the new chromene and chromane derivatives was investigated by means of component analysis [55]. Accordingly, a per residue binding free energy decomposition was performed exploiting the MD trajectory of ligand/σ_1 complex. This analysis was carried out using the MM/GBSA approach [56] and was based on the same snapshots used in the binding free energy calculation.

The entire computational procedure was optimized by integrating AMBER 12 in modeFRONTIER, a multidisciplinary and multi-objective optimization and design environment [57].

Acknowledgment

This work was done within the framework of the NRW International Graduate School of Chemistry, Münster, which is funded by the Government of the state Nordrhein-Westfalen and Westfälische Wilhelms-University Münster. The financial support is deeply acknowledged.

Appendix A. Supplementary data

Supplementary data related to this article can be found at http://dx.doi.org/10.1016/j.ejmech.2014.06.054.

References

[1] W.R. Martin, C.G. Eades, J.A. Thompson, R.E. Huppler, P.E. Gilbert, J. Pharmacol. Exp. Ther. 197 (1976) 517–532.
[2] S.W. Tam, Proc. Natl. Acad. Sci. U. S. A. 80 (1983) 6703–6707.
[3] D.B. Vaupel, Eur. J. Pharmacol. 92 (1983) 269–274.
[4] R. Quirion, W.D. Bowen, Y. Itzhak, J.L. Junien, J.M. Musacchio, R.B. Rothman, T.P. Su, S.W. Tam, D.P. Taylor, Trends Pharmacol. Sci. 13 (1992) 85–86.
[5] W.B. Bowen, Helv. Pharma. Acta 74 (2000) 211–218.
[6] M. Hanner, F.F. Moebius, A. Flandorfer, H.G. Knaus, J. Striessnig, E. Kempner, H. Glossmann, Proc. Natl. Acad. Sci. U. S. A. 93 (1996) 8072–8077.
[7] T. Hayashi, T.P. Su, J. Pharmacol. Exp. Ther. 306 (2003) 718–725.
[8] T. Hayashi, T.P. Su, Cell 131 (2007) 596–610.
[9] T.P. Su, T. Hayashi, T. Maurice, S. Buch, A.E. Ruoho, Trends Pharmacol. Sci. 31 (2010) 557–558.
[10] R.A. Wilke, R.P. Mehta, P.J. Lupardus, Y. Cben, A.E. Ruoho, M.B. Jackson, J. Biol. Chem. 274 (1999) 18387–18392.
[11] M. Johannessen, S. Ramachandran, L. Riemer, A. Ramos-Serrano, A.E. Ruoho, M.B. Jackson, Am. J. Physiol. Cell Physiol. 296 (2009) C1049–C1057.
[12] H. Zhang, J. Cuevas, J. Neurophysiol. 87 (2002) 2867–2879.
[13] P.D. Lupardus, R.A. Wilke, E. Aydar, C.P. Palmer, Y. Chen, A.E. Ruoho, M.B. Jackson, J. Physiol. 526 (2000) 527–539.
[14] F.P. Monnet, G. Debonnel, J. Junien, C. De Montigny, Eur. J. Pharmacol. 179 (1990) 441–445.
[15] T. Hayashi, T.P. Su, CNS Drugs 18 (2004) 269–284.
[16] E.J. Cobos, J.M. Entrena, F.R. Nieto, C.M. Cendan, E. DelPezo, Curr. Pharmacol. 6 (2008) 344–366.
[17] T. Maurice, T.P. Su, Pharmacol. Ther. 124 (2009) 195–206.
[18] M. Ishikawa, K. Hashimoto, J. Recept. Ligand Channel Res. 3 (2010) 25–36.
[19] J.M. Entrena, E.J. Cobos, F.R. Nieto, C.M. Cendan, G. Gris, E. Del Pozo, D. Zampanillo, J.M. Baeyens, Pain 143 (2009) 252–261.
[20] J.L. Diaz, D. Zamanillo, J. Corbera, J.M. Baeyens, R. Maldonado, M.A. Pericas, J.M. Vela, A. Torrens, Cent. Nerv. Syst. Agents Med. Chem. 9 (2009) 172–183.
[21] J.L. Diaz, R. Cuberes, J. Berrocal, M. Contijoch, U. Christmann, A. Fernández, A. Port, J. Holenz, H. Buschmann, C. Laggner, M.T. Serafini, J. Burgeno, D. Zamanillo, M. Merlos, J.M. Vela, C. Almansa, J. Med. Chem. 55 (2012) 8211–8224.
[22] B. Wünsch, J. Med. Chem. 55 (2012) 8209–8210.
[23] R.A. Glennon, S.Y. Ablordeppey, A.M. Ismaiel, M.B. El-Ashmawy, J.B. Fischer, K.B. Howie, J. Med. Chem. 37 (1994) 1214–1219.
[24] R.A. Glennon, Mini Rev. Med. Chem. 5 (2005) 927–940.
[25] B. Wünsch, Curr. Pharm. Des. 18 (2012) 930–937.
[26] E. Große Maestrup, C. Wiese, D. Schepmann, P. Brust, B. Wünsch, Bioorg. Med. Chem. 19 (2011) 393–405.
[27] C.A. Maier, B. Wünsch, J. Med. Chem. 45 (2002) 438–448.
[28] T. Schläger, D. Schepmann, K. Lehmkuhl, J. Holenz, J.M. Vela, H. Buschmann, B. Wünsch, J. Med. Chem. 54 (2011) 6704–6713.
[29] C. Oberdorf, D. Schepmann, J.M. Vela, J.L. Diaz, J. Holenz, B. Wünsch, J. Med. Chem. 51 (2008) 6531–6537.
[30] E. Laurini, V. Dal Col, S. Pricl, B. Wünsch, Bioorg. Med. Chem. Lett. 23 (2013) 2868–2871.
[31] J. Xu, C. Zeng, W. Chu, F. Pan, J.M. Rothfuss, F. Zhang, Z. Tu, D. Zhou, D. Zeng, S. Vangveravong, F. Johnston, D. Spitzer, K.C. Chang, R.S. Hotchkiss, W.G. Hawkins, K.T. Wheeler, R.H. Mach, Nat. Commun. 2 (2011) 380.
[32] K.W. Crawford, W.D. Bowen, Cancer Res. 1 (2002) 313–322.
[33] D. Harel, D. Schepmann, H. Prinz, R. Brun, J.T. Schmidt, B. Wünsch, J. Med. Chem. 56 (2013) 7442–7448.
[34] D. Harel, D. Schepmann, R. Brun, J.T. Schmidt, B. Wünsch, Org. Biomol. Chem. 11 (2013) 7342–7349.
[35] C. Meyer, D. Schepmann, S. Yanagisawa, J. Yamaguchi, V. Dal Col, E. Laurini, K. Itami, S. Pricl, B. Wünsch, J. Med. Chem. 55 (2012) 8047–8065.
[36] C.A. Maier, B. Wünsch, J. Med. Chem. 45 (2002) 4923–4930.
[37] C. Meyer, B. Neue, D. Schepmann, S. Yanagisawa, J. Yamaguchi, E.-U. Würthwein, K. Itami, B. Wünsch, Bioorg. Med. Chem. 21 (2013) 1844–1856.
[38] E. Laurini, V. Dal Col, M.G. Mamolo, D. Zampieri, P. Posocco, M. Fermeglia, L. Vio, S. Pricl, ACS Med. Chem. Lett. 2 (2011) 834–839.
[39] E. Laurini, D. Marson, V. Dal Col, M. Fermeglia, M.G. Mamolo, D. Zampieri, L. Vio, S. Pricl, Mol. Pharm. 9 (2012) 3107–3126.
[40] M.M.A. Bradford, Anal. Biochem. 72 (1976) 248–254.
[41] C. Stoscheck, Methods Enzym. 182 (1990) 50–68.
[42] Y.C. Cheng, W.H. Prusoff, Biochem. Pharmacol. 22 (1973) 3099–3108.
[43] D.L. DeHaven-Hudkins, L.C. Fleissner, F.Y. Ford-Rice, Eur. J. Pharmacol. Mol. Pharmacol. Sect. 227 (1992) 371–378.
[44] H. Mach, C.R. Smith, S.R. Childers, Life Sci. 57 (1995) PL-57–PL-62.
[45] D.A. Case, T.A. Darden, T.E. Cheatham III, et al., Amber 12, University of California, San Francisco, USA, 2012.
[46] E.F. Pettersen, T.D. Goddard, C.C. Huang, et al., J. Comput. Chem. 25 (2004) 1605–1612.
[47] W.L. Jorgensen, J. Chandrasekhar, J.D. Madura, et al., J. Chem. Phys. 79 (1983) 926–935.
[48] R.J. Loncharich, B.R. Brooks, R.W. Pastor, Biopolymers 32 (1992) 523–535.
[49] J.P. Ryckaer, G. Ciccotti, H.J.C. Berendsen, J. Comput. Phys. 23 (1977) 327–341.
[50] A. Toukmaji, C. Sagui, J. Board, et al., J. Chem. Phys. 113 (2000) 10913–10927.
[51] J. Srinivasan, T.E. Cheatham III, P. Cieplak, et al., J. Am. Chem. Soc. 120 (1998) 9401–9409.
[52] P.A. Kollman, I. Massova, C. Reyes, et al., Acc. Chem. Res. 33 (2000) 889–897.
[53] (a) D.L. Gibbons, S. Pricl, P. Posocco, E. Laurini, M. Fermgeglia, H. Sun, M. Talpaz, N. Donato, A. Quintas-Cardama, Proc. Natl. Acad. Sci. U. S. A. 111 (2014) 3550–3555;
(b) E. Laurini, P. Posocco, M. Fermeglia, D.L. Gibbons, A. Quintás-Cardama, S. Pricl, Mol. Oncol. 7 (2013) 968–975;
(c) D. Rossi, A. Pedrali, R. Gaggeri, A. Marra, L. Pignataro, E. Laurini, V. Dal Col, M. Fermeglia, S. Pricl, D. Schepmann, B. Wünsch, M. Peviani, D. Curti, S. Collina, Chem. Med. Chem. 8 (2014) 1514–1527;
(d) D. Rossi, A. Marra, P. Picconi, M. Serra, L. Catenacci, M. Sorrenti, E. Laurini, M. Fermeglia, S. Pricl, S. Brambilla, N. Almirante, M. Peviani, D. Curti, S. Collina, Bioorg. Med. Chem. 21 (2013) 2577–2586.
[54] I. Andricioaei, M. Karplus, J. Chem. Phys. 115 (2001) 6289–6292.
[55] H. Gohlke, C. Kiel, D.A. Case, J. Mol. Biol. 330 (2003) 891–913.
[56] V. Tsui, D.A. Case, Biopolymers 56 (2000) 75–291.
[57] http://www.esteco.com/home/mode_frontier/mode_frontier.html.